

The SNR of a Transit

David Kipping¹*

¹*Dept. of Astronomy, Columbia University, 550 W 120th Street, New York NY 10027*

Accepted 2023 May 7. Received 2023 May 2; in original form 2023 April 5

ABSTRACT

Accurate quantification of the signal-to-noise ratio (SNR) of a given observational phenomenon is central to associated calculations of sensitivity, yield, completeness and occurrence rate. Within the field of exoplanets, the SNR of a transit has been widely assumed to be the formula that one would obtain by assuming a boxcar light curve, yielding an SNR of the form $(\delta/\sigma_0)\sqrt{D}$. In this work, a general framework is outlined for calculating the SNR of any analytic function and it is applied to the specific case of a trapezoidal transit as a demonstration. By refining the approximation from boxcar to trapezoid, an improved SNR equation is obtained that takes the form $(\delta/\sigma_0)\sqrt{(T_{14} + 2T_{23})/3}$. A solution is also derived for the case of a trapezoid convolved with a top-hat, corresponding to observations with finite integration time, where it is proved that SNR is a monotonically decreasing function of integration time. As a rule of thumb, integration times exceeding $T_{14}/3$ lead to a 10% loss in SNR. This work establishes that the boxcar transit is approximate and it is argued that efforts to calculate accurate completeness maps or occurrence rate statistics should either use the refined expression, or even better numerically solve for the SNR of a more physically complete transit model.

Key words: eclipses — planets and satellites: detection — methods: statistical — methods: analytical

1 WHY SNR MATTERS

The expected signal-to-noise ratio (SNR) of a given observational phenomenon is central to discussions of experimental sensitivity, anticipated yield, completeness calculations and occurrence rate inferences. One might naively assume that the SNR of an exoplanetary transit would have a rather trivial formula, since the transit looks ostensibly similar to a boxcar function. Indeed, the first transit detection algorithm to gain widespread use, the Box-fitting Least Squares (BLS) algorithm (Kovács, Zucker, & Mazeh 2002), explicitly assumes as such, as well as papers outlining transit surveys, such as *Kepler* (Borucki et al. 2006). Under this assumption, the SNR of a single transit takes the form

$$\text{SNR} \propto \delta\sqrt{D}, \quad (1)$$

where δ is the transit depth and D is the duration of the boxcar transit, although sometimes the duration is replaced with the number of points occurring in transit, or something similar (e.g. Borucki et al. 2006). The constant of proportionality here concerns the noise and varies amongst authors depending on their specific treatment.

In the early years of transit surveys, there was arguably less motivation to skeptically challenge the boxcar assumption; afterall, the field was in “gold-rush” mode and it was not a critical issue if yield estimates were x2 off, or if BLS missed a few planets here and there. But in the *Kepler*-era, occurrence rate inferences became of central interest; a calculation which is predicated upon accurate completeness calculations (e.g. Petigura, Howard, & Marcy 2013; Dressing & Charbonneau 2013; Burke et al. 2015).

“Completeness” refers to the true positive rate of a survey, and within the transit literature is usually framed as the completeness conditional upon the fact that the planet in question has the correct geometry to transit (which means the geometric factor is treated separately). Given this framing, completeness is solely dependent upon the SNR of the signal in question - the higher the SNR, the higher the expected completeness.

Some of the earliest occurrence rate calculations assumed that the completeness was a Heaviside step function with respect to SNR. For example, Howard et al. (2012) assumed that all transits with $\text{SNR} > 10$ have 100% completeness. Fressin et al. (2013) introduced the more sophisticated linear-ramp model, where completeness was 0% up to some lower threshold SNR, then linearly ramped up to 100% where it saturated. Christiansen et al. (2013) advanced this

* E-mail: dkipping@astro.columbia.edu

further still, matching injection recovery simulations to a continuous, smooth inverse gamma cumulative density function. Modern calculations (e.g. see [Hsu et al. 2019](#)) often calculate completeness scores bespoke to each target ([Burke & Catanzarite 2017](#)). Regardless, at the core of all of these approaches is an SNR calculation. For example, if we took a given time series with stationary noise, and injected two different planets but with the same SNR, they should have the same completeness.

Clearly, an accurate SNR calculation is an essential ingredient, yet this term has received minimal attention compared to the parameterisation of the completeness curve. Indeed, even relatively modern *Kepler* occurrence rate calculations still explicitly adopt a SNR formula that implicitly assumes a boxcar transit. For example, see Equation (8) of [Hardegree-Ullman et al. \(2019\)](#) and Equation (4) of [Hsu et al. \(2019\)](#). The issue is likely even more widespread as authors don't always state how they define SNR in similar studies (e.g. [Grunblatt et al. 2019](#)).

Besides from occurrence rate calculations, the boxcar approximation is also widely assumed in survey yield calculations. For example, [Beatty & Gaudi \(2008\)](#) explicitly state that a boxcar model is assumed (see text below their Equation 4), an assumption also present in [Sullivan et al. \(2015\)](#) (see second sentence of their Section 6) and [Barclay, Pepper, & Quintana \(2018\)](#) (see their Equation 2).

The precise consequences of making this simplifying assumption upon these yield and occurrence rate calculations is non-trivial and beyond the scope of this work, but we can be certain that no exoplanet truly produces a boxcar transit. In this work, we ask then - what is the SNR of a transit?

Section 2 describes a general framework for calculating SNR. Section 3 (4) applies this to the specific case of a (convolved) trapezoidal light curve, rather than a limb darkened [Mandel & Agol \(2002\)](#) light curve. Despite this limitation, our work shows that even this is sufficient to establish that boxcar transit approximation should not be used and Section 5 expands upon this by discussing numerical approaches that can be used in real world cases.

2 A RIGOROUS DEFINITION FOR SNR

Chi-squared (χ^2) is a foundational concept in the statistical assessment of fit quality, applicable for independent normally distributed noise. The χ^2 metric is defined as the sum of the squares of the normalised residuals, where the residuals here are the differences between the data (\mathbf{y}) and some hypothesised model ($f[\mathbf{t}]$), with the normalisation being with respect to measurement uncertainties (σ):

$$\chi^2 = \sum_{j=1}^n \left(\frac{y_j - f[t_j]}{\sigma_j} \right)^2. \quad (2)$$

By construction, it only makes sense to speak of a χ^2 conditional upon some model. For data of length $n = 1$, it's easy to see how this means that $\sqrt{\chi^2}$ is the absolute difference between the model and the data in units of sigma (the standard error). And indeed, that statement effectively holds for any n , and the net number of sigmas deviance between the model and the data is $\sqrt{\chi^2}$.

With this in mind, we can employ a SNR definition that

equals the number of sigmas deviance between a hypothesised model, \mathbb{M} , and a null model, \mathbb{N} . We emphasise that this definition treats SNR as an act of model comparison. But ultimately, all detections are in fact an act of model comparison, something easy to forget since often we negate to articulate the tacit null model. To use an analogy, how can one ever measure the height of a mountain unless one compares it to some contextual plain? In this definition, our SNR becomes

$$\text{SNR}_{\Delta\chi^2} = \sqrt{\chi_{\mathbb{N}}^2 - \chi_{\mathbb{M}}^2}. \quad (3)$$

Whilst the above offers a conceptual outline of the relationship between SNR and χ^2 , a more rigorous justification is provided in [Scharf \(1991\)](#) and [Haykin \(1994\)](#). It's worth highlighting that this is hardly a novel statement, even within the field of exoplanets, for example [Zakamska, Pan, & Ford \(2011\)](#) define SNR using the same principle concerning simulated radial velocity observations.

2.1 From the hypothesized model

Consider the χ^2 resulting from model \mathbb{M} first, which predicts the \mathbf{y} data to be described by $f_{\mathbb{M}}[\mathbf{t}]$. In both this subsection and the next, we will assume that the data is distributed as $y_j \sim \mathcal{N}(f_{\mathbb{M}}[t_j], \sigma_j)$ i.e. the data is normally distributed about the hypothesised model. This is an ideal case where the fit model and the generative model are the same i.e. we are using the correct model. The presence of any latent unmodelled processes would naturally attenuate the SNR presented here.

In what follows, we derive the expectation value for the χ^2 arising from the null model. This is a standard and well-known derivation (e.g. see [Bain & Engelhardt 1992](#); [Grimmett & Stirzaker 2001](#)), but we walk through it here for the pedagogical clarity and to allow us to maintain a consistent notation system throughout.

Let us define the residuals resulting from the proposed model, \mathbb{M} as $\mathbf{r}_{\mathbb{M}}$, for which we can now state that $r_{\mathbb{M},j} \sim \mathcal{N}(0, \sigma_j)$. If we further define that the normalized residuals are given by $\rho_{\mathbb{M},j} = (r_{\mathbb{M},j}/\sigma_j)$, then it follows that $\rho_{\mathbb{M},j} \sim \mathcal{N}(0, 1)$ i.e. a standard normal. We may now write that the square of the normalized residual is given by $u_{\mathbb{M},j} = \rho_{\mathbb{M},j}^2$ as an intermediate step towards $\chi_{\mathbb{M}}^2 (= \sum u_{\mathbb{M},j})$. Because of the square, there are two roots for $\rho_{\mathbb{M},j}$, specifically $\rho_{\mathbb{M},j} = \pm\sqrt{u_{\mathbb{M},j}}$, and thus this factor needs to be accounted for when we transform the $\text{Pr}(\rho_{\mathbb{M},j})$ distribution to $\text{Pr}(u_{\mathbb{M},j})$, such that

$$\text{Pr}(u_{\mathbb{M},j}) du_{\mathbb{M},j} = 2\text{Pr}(\rho_{\mathbb{M},j}) \left| \frac{d\rho_{\mathbb{M},j}}{du_{\mathbb{M},j}} \right| du_{\mathbb{M},j}. \quad (4)$$

Since $d\rho_{\mathbb{M},j}/du_{\mathbb{M},j} = \frac{1}{2}u_{\mathbb{M},j}^{-1/2}$ and $\text{Pr}(\rho_{\mathbb{M},j}) = \frac{1}{\sqrt{2\pi}} \exp(-\frac{1}{2}\rho_{\mathbb{M},j}^2)$ (a standard normal) then this yields

$$\text{Pr}(u_{\mathbb{M},j}) = \frac{1}{\sqrt{2\pi u_{\mathbb{M},j}}} \exp\left(-\frac{u_{\mathbb{M},j}}{2}\right), \quad (5)$$

which is the chi-squared distribution for one degree of freedom. To go from $u_{\mathbb{M},j} \rightarrow \sum u_{\mathbb{M},j} (= \chi_{\mathbb{M}}^2)$ we need to add the random variates together. This can be achieved by noting that the distribution describing the sum of variates has a

characteristic function equal to the product of the characteristic functions from the individual variates being summed. As a first step towards this goal, the characteristic function of $\text{Pr}(u_{\mathbb{M},j})$ is found through a Fourier transform:

$$\begin{aligned}\phi_{\mathbb{M},j} &= \int_0^\infty \text{Pr}(u_{\mathbb{M},j}) \exp(iu_{\mathbb{M},j}t) du_{\mathbb{M},j}, \\ &= \frac{1}{\sqrt{1-2it}}.\end{aligned}\quad (6)$$

Accordingly, the characteristic function of $\text{Pr}(\chi_{\mathbb{M}}^2)$ is given by

$$\begin{aligned}\Phi_{\mathbb{M}} &= \prod_{j=1}^n \phi_{\mathbb{M},j}, \\ &= (1-2it)^{-n/2}.\end{aligned}\quad (7)$$

One could transform back to the probability density function for $\chi_{\mathbb{M}}^2$ at this point, using an inverse Fourier transform; however, in this work we really only care about the expectation value of $\chi_{\mathbb{M}}^2$ ($= \mathbb{E}[\chi_{\mathbb{M}}^2]$). This can be found by simply calculating the first raw moment of the distribution, which is given by

$$\begin{aligned}\mathbb{E}[\chi_{\mathbb{M}}^2] &= \left. \frac{\partial \Phi_{\mathbb{M}}}{\partial(it)} \right|_{t=0} \\ &= n.\end{aligned}\quad (8)$$

This result slightly differs from the more conventional framing of χ^2 as having a mean at the # of degrees of freedom ($= \#$ of data points - $\#$ of free parameters), whereas here n is just the number of data points. That's because our framing of the problem here does not involve a regression (hence there's no defined value of $\#$ of free parameters anyway). Instead, we are calculating the expectation value of the probability distribution for the normalised residuals, where the residuals are defined as the difference between the data and the *generative model* (rather than a *regressed model*). In the limit of large data ($n \gg 1$), which we adopt in this work, the definitions are of course equivalent and this follows from the fact that the regression will asymptotically approach the truth in this limit. It's somewhat advantageous to frame the problem in this way to generalise our work to non-linear models (such as a transit model, including even the box-car simplification scheme) for which the number of free parameters is ill-defined (Andrae, Schulze-Hartung, & Melchior 2010), or indeed linear models for which the basis functions are not linearly independent or have influential priors.

2.2 From the null model

We now proceed to calculate the mean χ^2 resulting from the null model i.e. $\chi_{\mathbb{N}}^2$. Let $r_{\mathbb{N},j} = (y_j - f_{\mathbb{N}}[t_j])$ be the residuals between the data and the null model. Recall that $y_j \sim \mathcal{N}(f_{\mathbb{M}}[t_j], \sigma_j)$, which means that $r_{\mathbb{N},j} \sim \mathcal{N}(f_{\mathbb{M}}[t_j] - f_{\mathbb{N}}[t_j], \sigma_j)$.

We can make further progress by normalizing by σ_j as before, such that $\rho_{\mathbb{N},j} = r_{\mathbb{N},j}/\sigma_j$, and thus allowing us to write that $\rho_{\mathbb{N},j} \sim \mathcal{N}(\Delta_j, 1)$, where we define $\Delta_j = (f_{\mathbb{M}}[t_j] - f_{\mathbb{N}}[t_j])/\sigma_j$.

With the probability distribution for $\rho_{\mathbb{N},j}$ obtained, we

can now transform to that for $u_{\mathbb{N},j} = \rho_{\mathbb{N},j}^2$ similar to before, but instead of obtaining the chi-squared distribution with one degree of freedom, this defines the *non-central* chi-squared distribution with one degree of freedom - and a non-centrality parameter given by Δ_j^2 :

$$\text{Pr}(u_{\mathbb{N},j}) = \frac{1}{\sqrt{2\pi u_{\mathbb{N},j}}} \exp\left(\frac{-u_{\mathbb{N},j}^2 - \Delta_j^2}{2}\right) \cosh(\sqrt{u_{\mathbb{N},j}} \Delta_j) \quad (9)$$

The characteristic function of the non-central chi-squared distribution of one degree of freedom is given by

$$\phi_{\mathbb{N},j} = \frac{1}{\sqrt{1-2it}} \exp\left(\frac{it\Delta_j^2}{1-2it}\right). \quad (10)$$

From this, the characteristic function for $\chi_{\mathbb{N}}^2$ is

$$\Phi_{\mathbb{N}} = \sum_{j=1}^n \phi_{\mathbb{N},j}. \quad (11)$$

Differentiating to obtain the first moment as before, which here now equals $\mathbb{E}[\chi_{\mathbb{N}}^2]$, we obtain

$$\mathbb{E}[\chi_{\mathbb{N}}^2] = n + \sum_{j=1}^n \Delta_j^2. \quad (12)$$

2.3 The SNR for Continuous Functions

The SNR can now be calculated by our definition earlier in Equation (3). Specifically, we have

$$\begin{aligned}\text{SNR}_{\Delta\chi^2} &= \sqrt{\sum_{j=1}^n \Delta_j^2}, \\ &= \sqrt{\sum_{j=1}^n \left(\frac{f_{\mathbb{M}}[t_j] - f_{\mathbb{N}}[t_j]}{\sigma_j} \right)^2}.\end{aligned}\quad (13)$$

Whilst the above is fairly intuitive, it's also somewhat limited in being dependent upon choices regarding cadence and sampling. The final step is to now generalise the above to an arbitrary continuous function (although in our case we care about the transit function specifically). To do so, let us assume that the sampling is regular with no data gaps, no read time (such that exposure time equals cadence) and is also homoscedastic. We further assume that the sampling is sufficiently dense that we can ignore the effect of the phasing of the data itself with respect to the mid-transit time. Since the uncertainty on the data will depend on possible binning choices, we define the uncertainty expected over one unit of time as σ_0 . By Poisson statistics, the uncertainty over three units of time will this be $\sigma_0/\sqrt{3}$, or more generally the uncertainty over a time δt cadence will be $\sigma_0/\sqrt{\delta t}$, such that

$$\begin{aligned}\text{SNR}_{\Delta\chi^2} &= \sqrt{\sum_{j=1}^n \Delta_j^2}, \\ &= \sqrt{\sum_{j=1}^n \left(\frac{f_{\mathbb{M}}[t_j] - f_{\mathbb{N}}[t_j]}{\sigma_0} \right)^2 \delta t}.\end{aligned}\quad (14)$$

In the limit of infinitesimal δt , this becomes

$$\text{SNR}_{\Delta\chi^2} = \sqrt{\int_{t_1}^{t_2} \left(\frac{f_{\mathbb{M}}[t] - f_{\mathbb{N}}[t]}{\sigma_0} \right)^2 dt}, \quad (15)$$

where $(t_2 - t_1)$ is the total temporal length of observations.

2.4 Modification for Linear Regression Problems

In the real world, the exact generative model behind the data is unknown to us, and indeed inaccessible. However, if at least the parametric form of the model is known, then the regressed model will tend towards the truth asymptotically as the data accumulates. Nevertheless, let us revisit our earlier assumption concerning this point. For a linear model, with no priors and a full rank design matrix, regression of said model to data will not result in $\mathbb{E}[\chi_{\mathbb{M}}] = n$, but rather $\mathbb{E}[\chi_{\mathbb{M}}] = n - k$, where k is the rank of the design matrix (Andrae, Schulze-Hartung, & Melchior 2010). We highlight that whether the transit model be Mandel & Agol (2002), a trapezoid or even a box-car, none of them are linear models and what follows is not actually applicable to the transit scenario. Regardless, let us proceed to gain some insights about the consequences of this earlier assumption.

From Equation (12), one can see that nominally the expected χ^2 value is the n plus the sum of the square deviances between the model being tested (in that case the null model) and the generative model. If the model being tested is the generative model, then the deviances are zero and hence Equation (12) becomes Equation (8). Accordingly, this means that the expected chi-squared values get modified, in the case of regression, to

$$\begin{aligned} \chi_{\mathbb{M}}^2 &\rightarrow n - k_{\mathbb{M}}, \\ \chi_{\mathbb{N}}^2 &\rightarrow n - k_{\mathbb{N}} + \sum_{j=1}^n \Delta_j^2, \end{aligned} \quad (16)$$

where $k_{\mathbb{M}}$ is the rank of the design matrix for model $f_{\mathbb{M}}[t]$ and $k_{\mathbb{N}}$ is that for model $f_{\mathbb{N}}[t]$. The modification to our SNR equation is then simply

$$\text{SNR}_{\Delta\chi^2} = \sqrt{(k_{\mathbb{N}} - k_{\mathbb{M}}) + \int_{t_1}^{t_2} \left(\frac{f_{\mathbb{M}}[t] - f_{\mathbb{N}}[t]}{\sigma_0} \right)^2 dt}. \quad (17)$$

Since one usually would have $k_{\mathbb{M}} > k_{\mathbb{N}}$, the new term included is negative and thus serves as a penalty to the SNR. This again reinforces our claim that the SNR derived in the previous subsection and presented in Equation (15) is an idealised, upper-limit on SNR.

3 THE SNR OF A TRAPEZOIDAL TRANSIT

3.1 The Double Box (BB) Approximation

To zeroth order approximation, the shape of a transit light is a box and the appeal of this model is undoubtedly borne of its simplicity. Let us call this the double box (BB) approximation due its double appearance in that statement; both as the assumed generative model and the model employed to

define SNR. The fact that our generative model is here assumed to be a box immediately makes it incongruous with this section, whose title clearly seeks the SNR of a *trapezoidal* transit. Nevertheless, let us continue with this case for the moment as it provides some context for what follows and helps us understand the origin of the most commonly cited formulae for transit SNR.

In this scenario, it is straight-forward to calculate the SNR. Let us begin by first defining the transit model as a function of time from the mid-transit, t , writing the normalised intensity as a function of time as

$$f_{\text{B}}[t] = \begin{cases} 1 & \text{if } t \leq -D/2, \\ 1 - \delta & \text{if } -D/2 < t \leq D/2, \\ 1 & \text{if } t > D/2, \end{cases} \quad (18)$$

where δ is the depth of the transit and D is the duration of the box-car. Now it is necessary to define the SNR of this transit. The truth is that there's no single way to define SNR, and our exploration of the literature reveals it is rarely rigorously derived or even defined. In the case of the BB approximation, however, two reasonable proposals yield the same result, which ultimately stem from the self-consistency of the double box framework. The first, and perhaps most common, is to define SNR as the depth divided by the error on the depth. So we now need expressions for each of these components.

Looking at the box-car function, Equation (18), one can re-arrange to solve for depth using $\delta = (\overline{I_{\text{out}}} - \overline{I_{\text{in}}})$, where $\overline{I_{\text{out}}}$ is the mean out-of-transit intensity and $\overline{I_{\text{in}}}$ is the mean in-transit intensity. In the more general case where we observe unnormalised intensities, this becomes

$$\Delta F_{\text{BB}} \equiv \frac{\overline{I_{\text{out}}} - \overline{I_{\text{in}}}}{\overline{I_{\text{out}}}}, \quad (19)$$

where i) δ is replaced with “ ΔF ” to define the flux change (which will be useful later to avoid notational confusion) and ii) the “BB” subscript is added to explicate the transit model was generated using a box-car function, Equation (18), and the depth is solved for assuming a boxcar function by inverting Equation (18).

Under the assumption of no time-correlated noise structure, the uncertainty on ΔF_{BB} will be

$$\begin{aligned} \sigma_{\Delta F_{\text{BB}}}^2 &= (\partial_{\overline{I_{\text{out}}}} \delta_{\text{BB}})^2 \sigma_{\overline{I_{\text{out}}}}^2 + (\partial_{\overline{I_{\text{in}}}} \delta_{\text{BB}})^2 \sigma_{\overline{I_{\text{in}}}}^2, \\ &= \frac{\overline{I_{\text{out}}}^2 \sigma_{\overline{I_{\text{in}}}}^2 + \overline{I_{\text{in}}}^2 \sigma_{\overline{I_{\text{out}}}}^2}{\overline{I_{\text{out}}}^4}. \end{aligned} \quad (20)$$

To make progress, it is assumed that the noise is dominated by photon-noise and thus can apply Poisson noise statistics. In this case, if the noise per unit time is σ_0 , then the noise over an interval of D (the transit duration) will be $\sigma_{\overline{I_{\text{in}}}} = \sigma_0/\sqrt{D}$. Similarly, $\sigma_{\overline{I_{\text{out}}}} = \sigma_0/\sqrt{T_{\text{out}}}$, where T_{out} is the out-of-transit observational baseline. Now applying this to normalised intensities using Equation (18)

$$\text{SNR}_{\Delta F, \text{BB}} = \frac{\delta}{\sigma_0} \frac{1}{\sqrt{\frac{1}{D} + \frac{(1-\delta)^2}{T_{\text{out}}}}}, \quad (21)$$

and in the limit of large amounts of out-of-transit data

$$\lim_{T_{\text{out}} \rightarrow \infty} \text{SNR}_{\Delta F, \text{BB}} = \frac{\delta}{\sigma_0} \sqrt{D}. \quad (22)$$

An alternative definition for SNR is the $\text{SNR}_{\Delta\chi^2}$ formula presented earlier in Equation (15). Feeding Equation (18) into Equation (15), we obtain

$$\text{SNR}_{\Delta\chi^2} = \frac{\delta}{\sigma_0} \sqrt{D}, \quad (23)$$

i.e. the same result. This is not surprising given that model is completely defined by the step function in intensity and we are here comparing the same model as the generative one. As an aside, it is noted that if one phase-folds N transits together (or equivalently regresses a multi-epoch light curve model to N transits), then $\sigma_0 \rightarrow \sigma_0/\sqrt{N}$.

Equation (22) is indeed the most commonly quoted definition for SNR of a transit. The obvious major drawback of this formula is that its underlying assumptions are patently wrong, a box-car transit is impossible (and has even been suggested as a technosignature given its impossibility; Kipping & Teachey 2016). It really doesn't mean much to speak of this SNR, since it corresponds to a case which never exists - a generative model equal to a box-car transit. In this sense, it cannot be compared to other SNRs values presented in the next two subsections, since they are for a distinct generative model (namely a trapezoid).

It is noted that this formula also appears in Carter et al. (2008), despite the fact the authors are considering the SNR of δ from a trapezoidal transit, not a boxcar. In that work, the authors refer to the SNR as “ Q ” and after notational translation have the same result, except that $D \rightarrow W$ which is not a general duration but fixed to the full width half maximum transit duration i.e.

$$W \equiv \frac{T_{14} + T_{23}}{2}. \quad (24)$$

3.2 The Trapezoid-Box (TB) Approximation

Things become more complicated when one considers the case where the assumed generative model is a trapezoid, but SNR is still in terms of a box - what it is dubbed here the trapezoid-box (TB) approximation. In this scenario, the generative model is now that of a trapezoid of full transit duration T_{14} and totality duration T_{23} :

$$f_{\text{T}}[t] = \begin{cases} 1 & \text{if } t \leq -T_{14}/2, \\ 1 - \frac{(2t+T_{14})\delta}{T_{14}-T_{23}} & \text{if } -T_{14}/2 < t \leq -T_{23}/2, \\ 1 - \delta & \text{if } -T_{23}/2 < t \leq T_{23}/2, \\ 1 + \frac{(2t-T_{14})\delta}{T_{14}-T_{23}} & \text{if } T_{23}/2 < t \leq T_{14}/2, \\ 1 & \text{if } t > T_{14}/2. \end{cases} \quad (25)$$

A basic issue now is that when placing a box over the trapezoid, SNR_{TB} must be sensitive to how big we make that box, i.e. the value of D . Whilst that was also true in the previous section, there was only really one obvious choice for D to set it to be equal to the duration used in the generative model i.e. D . But now the question arises, should $D = T_{23}$?

Or maybe T_{14} ? Or perhaps some combination of the two? In this sense, there is no single solution for SNR_{TB} .

A case study example of this comes from Kipping & Sandford (2016). In that work, I too casually suggested that SNR could be defined using the δ method applied to a trapezoid. Further, D was set to T_{14} . These were choices made by myself as the lead author and in hindsight they were made too hastily; but after all the process of science is one of continuous refinement, even in our own understanding. The choice of D sets what defines $\overline{I}_{\text{out}}$ and \overline{I}_{in} . Let's proceed first by keeping D general and following the ΔF method, such that

$$\overline{I}_{\text{in, TB}} = D^{-1} \int_{-D/2}^{D/2} f_{\text{T}}[t] dt \quad (26)$$

yielding

$$\overline{I}_{\text{in, TB}} = \begin{cases} 1 - \delta & \text{if } D \leq T_{23}, \\ 1 + \delta \left(\frac{T_{23}^2 - D(2T_{14} - D)}{2(T_{14} - T_{23})D} \right) & \text{if } T_{23} < D \leq T_{14}, \\ 1 - \delta \left(\frac{T_{14} + T_{23}}{2D} \right) & \text{if } D > T_{14}, \end{cases} \quad (27)$$

The mean out-of-transit intensity can be calculated in a similar way, but it's clear that the best case scenario will occur when it's simply taken to equal unity, thus maximising the ΔF . Similarly, the optimal choice of D must lie in the range $[T_{23}, T_{14}]$. Following the same steps as with $\text{SNR}_{\Delta F, \text{BB}}$, this ideal case leads to

$$\lim_{T_{\text{out}} \rightarrow \infty} \text{SNR}_{\Delta F, \text{TB}} = \left(\frac{D(2T_{14} - D) - T_{23}^2}{2D(T_{14} - T_{23})} \right) \left(\frac{\delta}{\sigma_0} \right) \sqrt{D}. \quad (28)$$

If we evaluate Equation (28) in the case of $D \rightarrow T_{14}$, we recover the SNR equation for a transit presented by Kipping & Sandford (2016) in their Equation (11):

$$\lim_{D \rightarrow T_{14}} \lim_{T_{\text{out}} \rightarrow \infty} \text{SNR}_{\Delta F, \text{TB}} = \left(\frac{T_{14} + T_{23}}{2\sqrt{T_{14}}} \right) \left(\frac{\delta}{\sigma_0} \right). \quad (29)$$

This reproduction of the Kipping & Sandford (2016) formula more clearly elucidates the derivation and thinking behind it. The assumption is that the generative model is a trapezoid, but the SNR is defined using a box-car delta-flux approach (hence a TB scenario) where $D = T_{14}$. However, one can actually increase the SNR here slightly by instead of setting $D = T_{14}$, optimising $\text{SNR}_{\Delta F, \text{TB}}$ with respect to D through differentiation, yielding an optimal D of

$$\hat{D}_{\Delta F} = \frac{T_{14} + \sqrt{T_{14}^2 + 3T_{23}^2}}{3}, \quad (30)$$

where the hat notation denotes an optimised value, and the subscript ΔF is added to emphasise that this is only demonstrated to be the optimal choice of D when using the ΔF method.

This result may be useful for those running BLS in archival data on signals of known T_{23} and T_{14} , where the optimal signal width should be set to the above to maximize SNR (Yao et al. 2019). At the optimal D , and in the limit of large T_{out} , one obtains

$$\lim_{D \rightarrow \hat{D}_{\Delta F}} \lim_{T_{\text{out}} \rightarrow \infty} \text{SNR}_{\Delta F, \text{TB}} = \left(\frac{2(-3T_{23}^2 + T_{14}(T_{14} + \sqrt{T_{14}^2 + 3T_{23}^2}))}{3\sqrt{3}(T_{14} - T_{23})\sqrt{T_{14}^2 + 3T_{23}^2}} \right) \times \left(\frac{\delta}{\sigma_0} \right). \quad (31)$$

It was verified that the same result is obtained if one does not assume $\overline{T_{\text{out}}} = 1$ but actually works through the cases, and of course the equivalence is not surprising since in the limit of $T_{\text{out}} \rightarrow \infty$ one necessarily has $\overline{T_{\text{out}}} \rightarrow 1$.

3.3 The Trapezoidal-Trapezoidal (TT) Approximation

Finally, let us consider the case where the generative model is a trapezoid and the model of comparison is also a trapezoid. The SNR cannot be computed using the ΔF method here, so instead we use the $\Delta\chi^2$ approach. Feeding Equation (25) into Equation (15), we obtain

$$\text{SNR}_{\Delta\chi^2, \text{TT}} = \sqrt{\frac{T_{14} + 2T_{23}}{3}} \left(\frac{\delta}{\sigma_0} \right). \quad (32)$$

This is actually a far easier calculation than TB, which is greatly complicated by the fact one is attempting to compare the wrong model to a generative function. Our expectation here should be that using the correct model will lead to a higher SNR, since otherwise one has a misspecified likelihood function and that will pull the SNR down. Although limb darkening and ingress/egress curvature are ignored here, largely because they are intractable to the analytic approach sought in this paper, the example of limb darkening exemplifies this via the Transit Least Squares (TLS) algorithm which achieves slightly improved sensitivity over BLS by merely employing an improved transit shape (Hippke & Heller 2019).

Figure 1 verifies our expectations, where one can see four versions of the SNR formulae applied to a trapezoid, three from the ΔF (TB) methods, and one from the $\Delta\chi^2$ (TT) method. Note how a BB formula is not shown here (box-car models applied to box-car generated transits) since this is conditioned upon a different data set (or really generative model) to begin with. The formulae all converge when $T_{14} \rightarrow T_{23}$, since in this limit the generative model becomes a box-car, and as shown earlier in Section 3.1 one finds perfect agreement between ΔF and $\Delta\chi^2$ methods here (since both are correctly specified models essentially). In all other cases though, the $\Delta\chi^2$ method yields the highest SNR. In other words, any other formulae is in fact underestimating the true SNR.

3.4 A Note on Grazing Transits

Having established that the $\Delta\chi^2$ method maximises SNR, let us now consider how to extend to grazing transit geometries. In this case, the impact parameter, b , lies in the range $(1-p) \leq b < (1+p)$, where $p \equiv (R_p/R_\star)$ is the ratio-of-radii. Accordingly, $T_{23} \rightarrow 0$ but T_{14} remains positive. For a non-grazing geometry (and ignoring limb darkening as has been

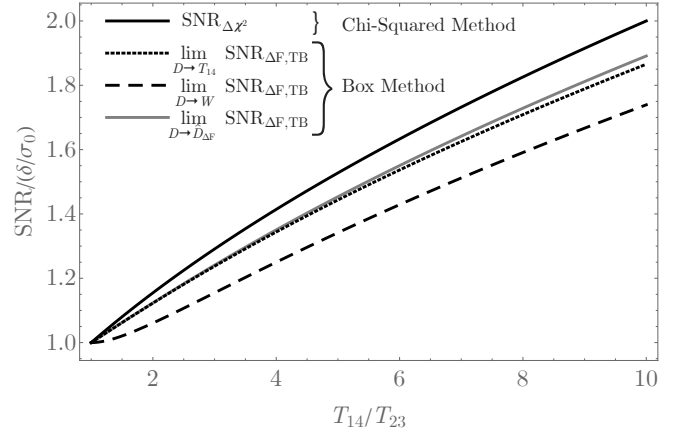


Figure 1. Comparison of four formulae for the SNR of a trapezoidal transit. The $\Delta\chi^2$ method is the only one that uses the correct model to describe the light curve shape, whereas ΔF (a box-car model) is always an approximation to the trapezoid only. As a result, it always produces worse SNRs than the $\Delta\chi^2$ method.

done throughout), $\delta = p^2$, but this breaks down for grazing cases, becoming (Mandel & Agol 2002)

$$\delta[p, b] = \begin{cases} p^2 & \text{if } 0 \leq b < 1 - p, \\ \frac{1}{\pi} \left(p^2 \kappa_0 + \kappa_1 - \sqrt{\frac{4b^2 - (1+b^2-p^2)^2}{4}} \right) & \text{if } 1 - p \leq b < 1 + p, \\ 0 & \text{if } 1 + p \leq b < \infty, \end{cases} \quad (33)$$

where

$$\kappa_0 = \cos^{-1} \left(\frac{p^2 + b^2 - 1}{2pb} \right), \quad (34)$$

$$\kappa_1 = \cos^{-1} \left(\frac{1 - p^2 + b^2}{2b} \right). \quad (35)$$

Thus, Equation (32) remains valid except that it is understood that δ is given by Equation (33) and $T_{23} \rightarrow 0$.

3.5 A Note On Multiple Transits

In the case of multiple transits, the analytic formulae presented thus far and throughout are easily modified such that $\sigma_0 \rightarrow \sigma_0/\sqrt{N}$, where N is the number of transits observed. As before, this assumes regular sampled, homoscedastic data. Real-world cases affected by partial transits, irregular/sparsely sampling and/or heteroscedastic data may need to instead numerically evaluate the SNR, as discussed earlier.

4 THE SINNING OF BINNING

4.1 The Effects of Binning

Photometric time series are not captured with exposures of infinitesimal duration. Each data point is an exposure of finite duration and during that exposure the light curve can change. What this means is that our observations are in fact

average intensities over the exposure times. If one phase-folds a large number of transits together with a certain exposure time, the resulting light curve will be distorted from the naive model one might expect ignoring this effect. Like a taking a photo of a racing car, the image appears blurred, smeared out; and so too is a transit. A transit is particularly susceptible to this because of its sharp discontinuities; observations captured near the first and fourth contact points for example will not exhibit the crisp discontinuity but rather a smoothed curve as a result of exposure time. It's important to emphasise that all observations are in fact binned like this; one cannot ever observe a transit with infinitesimal exposures.

This effect was first pointed out, in the case of transits, in Kipping (2010) with the moniker “binning is sinning”. And since then the effect has been demonstrated and explored for supernovae (Brout, Hinton, & Scolnic 2021) and phase curves (Morello, Dyrek, & Changeat 2022). In Kipping (2010), the effect was explored numerically. Trapezoidal transits were simulated, smoothed with a moving average filter, and then the consequences for parameter retrieval were discussed, as well presenting numerical schemes to compensate. A basic observation is that the observed first-to-fourth contact duration satisfies $T_{14,\text{obs}} = T_{14} + I$ and the observed second-to-third contact duration satisfies $T_{23,\text{obs}} = T_{23} - I$, where I is the exposure/integration time. But what is the SNR of this smeared out transit?

Since the contact points shift in/out by I , one might be tempted to use Equation (32) but simply apply the appropriate modification to T_{14} and T_{23} . But this is wrong! Inspection of Figure 1 of Kipping (2010) reveals why - it's not just that the contact points shift, the transit shape has changed from a trapezoid (characterised by straight lines) to a curved form i.e. $d^2f/dt \neq 0$. In other words, the generative model is no longer a trapezoid. So using a trapezoidal model to calculate the SNR of a non-trapezoidal shape is wrong, as was demonstrated in the last section.

What is needed is a closed-form expression for the shape of a trapezoidal transit in the presence of finite integration time. Kipping (2010) never presented such a formula, largely because it's cumbersome to calculate and was unnecessary to the point of that paper. But here, we cannot calculate the SNR of such a transit without it - at least not analytically.

4.2 The Convolved Transit

The solution to this is to consider what a finite exposure time does. Upon a phase-folded time series of transit observations, the finite exposure time effect acts as a moving average with a bandwidth of I . A moving average of some function, $f[t]$, is the convolution of $f[t]$ with a top-hat function, $g[x]$:

$$\begin{aligned} f'[t] &= f[t] \star g[t], \\ &= \int_{-\infty}^{\infty} f[u]g[t-u]du. \end{aligned} \quad (36)$$

This simple formula betrays the challenge of actually calculating this for a trapezoid, because the trapezoid is a piece-wise function and thus one has to essentially perform this convolution in a piece-meal manner. In fact, there are nine unique regimes, which are best illustrated in the case of

a short exposure time but the existence of nine regimes persists irrespective of I . If the mid-exposure/integration time is given by $t_{\mathcal{J}}$, then these are

- i) $-\infty < t_{\mathcal{J}} \leq t_1 - I/2$ (pre-transit),
- ii) $t_1 - I/2 < t_{\mathcal{J}} \leq t_1 + I/2$ (saddles 1st-contact),
- iii) $t_1 + I/2 < t_{\mathcal{J}} \leq t_2 - I/2$ (within ingress),
- iv) $t_2 - I/2 < t_{\mathcal{J}} \leq t_2 + I/2$ (saddles 2nd-contact),
- v) $t_2 + I/2 < t_{\mathcal{J}} \leq t_3 - I/2$ (within totality),
- vi) $t_3 - I/2 < t_{\mathcal{J}} \leq t_3 + I/2$ (saddles 3rd-contact),
- vii) $t_3 + I/2 < t_{\mathcal{J}} \leq t_4 - I/2$ (within egress),
- viii) $t_4 - I/2 < t_{\mathcal{J}} \leq t_4 + I/2$ (saddles 4th-contact),
- ix) $t_4 + I/2 < t_{\mathcal{J}} \leq \infty$ (post-transit).

One can now see what we mean by “small” I ; it really defines the integration time being less than any relevant timescale here, so smaller than T_{23} (which is necessarily smaller than T_{14}) and also smaller than the ingress/egress time. Thus, the “small” I regime is characterised by $0 < I < T_{23} < T_{14}$ and $I < (T_{14} - T_{23})/2$. In this regime, one can now proceed through each of the nine cases and compute the new convolved transit, $f'_T[t]$, using Equation (25) and

$$f'_T[t] = I^{-1} \int_{t_{\mathcal{J}}-I/2}^{t_{\mathcal{J}}+I/2} f_T[t] dt, \quad (37)$$

which simplifies Equation (36) to the case of a top-hat $g[t]$, as we have here. Besides from the small I regime, this work has identified five other regimes that each require a tailored treatment of both the nine cases and the resulting integrals. Including the small I regime, these are

- A) $0 < I < T_{23} < W < T_{14}$ and $0 < I < (T_{14} - T_{23})/2$ (small I)
- B) $0 < I < T_{23} < W < T_{14}$ and $0 < (T_{14} - T_{23})/2 < I$ (ingress enveloping I)
- C) $0 < T_{23} < I < W < T_{14}$ and $0 < I < (T_{14} - T_{23})/2$ (totality enveloping I)
- D) $0 < T_{23} < I < W < T_{14}$ and $0 < (T_{14} - T_{23})/2 < I$ (ingress-totality enveloping I)
- E) $0 < T_{23} < W < I < T_{14}$ [and $0 < (T_{14} - T_{23})/2 < I$] (FWHM enveloping I)
- F) $0 < T_{23} < W < T_{14} < I$ [and $0 < (T_{14} - T_{23})/2 < I$] (transit enveloping I)

For the last two regimes, the second condition is put in square parentheses to highlight that it's always satisfied given the first condition. One may now proceed through the 9×6 integrals by hand and evaluate each function, then stitch the results together into a piece-wise function. The final expression was graphically tested with live manipulate functions against numerically smoothed light curves. The results are presented in the Appendix for the sake of conciseness here. It is noted that cases 1) and 2) also appear in Equation (7) of Price & Rogers (2014), but they do not consider the longer I cases necessary to fully generalise the convolved transit.

4.3 When it comes to SNR, is binning sinning?

Equipped with our convolved transit expression, we can now finally come back to the topic at the core of this paper - what is the SNR? This is crucial question when it comes to the design of upcoming transit surveys, such as PLATO (Rauer et al. 2014). The advantage of binning time series into ever

coarser integrations is that less data needs to be stored and transmitted back to Earth from space-based missions, thus allowing a larger number of stars to be observed. The disadvantage of larger integration times is that one smears out the transit shape and thus have fundamentally lost information.

This loss of information has been demonstrated to cause a precision loss in the retrieved transit parameters (Price & Rogers 2014). On this basis, it stands to reason that the SNR will also be deteriorated due to the integration time effect. Using our expressions for the trapezoid light curve with smearing, one may evaluate the SNR rigorously using Equation (15), which yields the following piece-wise results:

$$\left(\frac{\text{SNR}'_{\Delta\chi^2,A}}{\delta/\sigma_0}\right)^2 = \left(5T_{23}I^2 - 5T_{14}(3T_{23}^2 + I^2) + 5T_{14}^3 + 10T_{23}^3 + 2I^3\right) / \left(15(T_{14} - T_{23})^2\right) \quad (38)$$

$$\left(\frac{\text{SNR}'_{\Delta\chi^2,B}}{\delta/\sigma_0}\right)^2 = \left(120T_{23}I^2 + T_{14}(20T_{23}I + 3T_{23}^2 + 120I^2) - 10T_{23}^2I - T_{14}^2(3T_{23} + 10I) + T_{14}^3 - T_{23}^3 - 80I^3\right) / \left(240I^2\right) \quad (39)$$

$$\left(\frac{\text{SNR}'_{\Delta\chi^2,C}}{\delta/\sigma_0}\right)^2 = \left(-5T_{14}I^4 + 5T_{14}^3I^2 - 5T_{23}^2I^2(3T_{14} - 2I) + 5T_{23}^4I - T_{23}^5 + 3I^5\right) / \left(15(T_{14} - T_{23})^2I^2\right) \quad (40)$$

$$\left(\frac{\text{SNR}'_{\Delta\chi^2,D}}{\delta/\sigma_0}\right)^2 = \left(-80T_{23}I^4 + 80T_{23}^2I^3 - 40T_{23}^3I^2 + 10T_{14}^3(4T_{23}I + T_{23}^2 + 12I^2) + 5T_{14}T_{23}(-24T_{23}I^2 + 8T_{23}^2I + T_{23}^3 + 32I^3) + 70T_{23}^4I - 10T_{14}^2(T_{23} + 2I)^3 - 5T_{14}^4(T_{23} + 2I) + T_{14}^5 - 17T_{23}^5 + 16I^5\right) / \left(240(T_{14} - T_{23})^2I^2\right) \quad (41)$$

$$\left(\frac{\text{SNR}'_{\Delta\chi^2,E}}{\delta/\sigma_0}\right)^2 = \left(10T_{14}^3(T_{23}^2 + 8I^2) - 20T_{14}^2(3T_{23}^2I + 4I^3) + 5T_{14}(T_{23}^4 + 8I^4) - 10T_{14}^4I + 30T_{23}^4I + T_{14}^5 - 8T_{23}^5 - 8I^5\right) / \left(120(T_{14} - T_{23})^2I^2\right) \quad (42)$$

$$\left(\frac{\text{SNR}'_{\Delta\chi^2,F}}{\delta/\sigma_0}\right)^2 = \left(T_{14}^2(30I - 14T_{23}) + T_{23}T_{14}(60I - 11T_{23}) + 30T_{23}^2I - 7T_{14}^3 - 8T_{23}^3\right) / \left(120I^2\right) \quad (43)$$

Rather than trying to gain insight from the equations themselves, it's far more intuitive to simply plot the smeared SNR as a function of integration time, as shown in Figure 2. Note that this figure normalises the smeared SNR by the

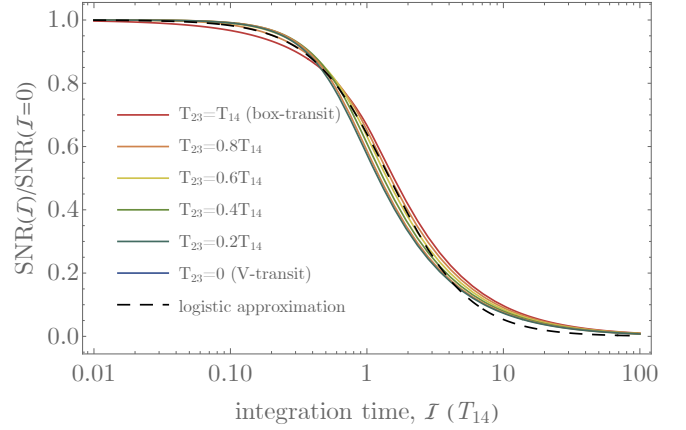


Figure 2. SNR of a trapezoidal transit with finite integration time, relative to the SNR found with infinitesimal integration time. As expected, integration time effects attenuate the transit SNR and can be well approximated by a logistic function given by Equation (44).

original expression found earlier ignoring this effect (Equation 32), since the depth and measurement uncertainty consistently cancel out in doing so. Thus, the loss in SNR is completely described by T_{14} , T_{23} and I . By working in units of T_{14} , one can further reduce the dimensionality to two. This is visualised by using the x-axis for one of these (I/T_{14}) and multiple colored lines for the other (T_{23}/T_{14}).

As expected, the SNR drops off smoothly and monotonically in all cases, providing some assurance that our piece-wise function correctly connects at the case boundaries, as well exhibiting the intuitive behaviour one expects of SNR dropping with ever larger I . Crucially, the SNR never drops to zero even at excessive large I values, although it does asymptotically approach zero (again as expected). It is also worth noting that the ensemble of models are in fairly good agreement with one another, and can be approximated by a single function shown in black, and given by

$$\frac{\text{SNR}(I)}{\text{SNR}(I=0)} \simeq \frac{1}{1 + \exp\left(-\frac{3}{2}(0.384363 - \log_e \frac{I}{T_{14}})\right)}. \quad (44)$$

The approximation dictates that one loses $\gtrsim 10\%$ of the SNR when $I \gtrsim T_{14}/3$, which serves as a useful rule of thumb to guide observers. In extreme cases, such as 30-minute *Kepler* long-cadence on a 1-minute white dwarf transit, the SNR loss is severe and drops to 1% of the unsmeared value.

4.4 A Note On Extreme Integration Times

Recall earlier in Section 2.3 how an underlying assumption of our analytic formulae is that the transit is well-sampled, which comes into question as the integration time increases. For sparsely sampled transits, the phasing of the points with respect to the transit mid-time will increasingly influence the resulting SNR. However, even when $\mathcal{J} \sim W$, the problem of special phasing arrangements washes out if $N \gg 1$, since the phase-folded transit will again have nearly uniform, regular sampling. In this sense, a single transit with sparse sampling

represents the most egregious violation of our sampling assumption.

5 BUT TRANSITS AREN'T TRAPEZOIDS!

This work has discussed how, within the existing exoplanet literature, the most commonly used formula for transit SNR is only accurate for box-shaped transits. Further, a transit can never be (naturally) box-shaped (Kipping & Teachey 2016). The box-shaped transit can perhaps be best described as a zeroth-order approximation of some physically motivated light curve (e.g. Mandel & Agol 2002), and in that vein a trapezoidal light curve is a refined approximation - but unquestionably still an approximation. In this sense, the new SNR formula presented in this work for a trapezoidal light curve is also an approximation (Equation 32), albeit an improved approximation upon the box.

So what if one wishes to go further and have a light curve model that correctly accounts for the ingress/egress area of overlap and/or limb darkening effects (Mandel & Agol 2002)? Or indeed, what if one wishes to use an even more sophisticated model than that; one which accounts for gravity darkening (Herman et al. 2018), planetary oblateness (Carter & Winn 2010), nightside pollution (Kipping & Tinetti 2010), atmospheric refraction (Sidis & Sari 2010) and indeed many other possible complications? In this work, the author was not able to find a closed-form SNR solution (using the integral of Equation 15) to even the relatively simple case of a non-limb darkened Mandel & Agol (2002) model and thus a trapezoidal transit may be the most accurate approximate model one can ever hope to have a closed form SNR transit equation for.

A closed-form solution like this certainly has its place though, and for surveys operating towards the infrared (where limb darkening is suppressed) it may be wholly appropriate. But in cases where more finesse is required, it is recommended to numerically evaluate the SNR of the transit model using Equation (15) for continuous functions in the presence of regularly sampled, homoscedastic data, or Equation (14) otherwise.

More broadly, this work establishes that the boxcar transit SNR is not magically equivalent to the trapezoidal case, nor indeed more nuanced transit models. So adopting the boxcar transit SNR comes at some finite loss in accuracy. Section 4 also establishes that using longer exposure/binning/integration times in a photometric survey will reduce the SNR of transits. The crucial timescale here is T_{14} . For integrations times much faster than this, the reduction is small, whereas for times longer than this, there is a dramatic decrease. This is particularly pertinent when considering the detection efficiency towards very short transients, such as white dwarf transiting planets (Vanderburg et al. 2020), whose transits typically last for mere minutes (Cortés & Kipping 2019). Even the “fast” 2-minute cadence of *TESS* (Ricker et al. 2015) is too slow to avoid substantial SNR loss here. Any effort at occurrence rate calculations for such transients (e.g. van Sluijs & Van Eylen 2018) must be careful to not only use a realistic astrophysical model, but also account for the convolutional smearing, which will surely require a numerical approach for full accuracy.

ACKNOWLEDGMENTS

Thank-you to the anonymous reviewer for their helpful review. This work was supported by patrons to the Cool Worlds Lab, for which the author thanks D. Smith, M. Sloan, C. Bottaccini, D. Daughaday, A. Jones, S. Brownlee, N. Kildal, Z. Star, E. West, T. Zajonc, C. Wolfred, L. Skov, G. Benson, A. De Vaal, M. Elliott, B. Daniluk, M. Forbes, S. Vystoropskyi, S. Lee, Z. Danielson, C. Fitzgerald, C. Souter, M. Gillette, T. Jeffcoat, J. Rockett, D. Murphree, S. Hannum, T. Donkin, K. Myers, A. Schoen, K. Dabrowski, J. Black, R. Ramezankhani, J. Armstrong, K. Weber, S. Marks, L. Robinson, S. Roulier, B. Smith, G. Canterbury, J. Cassese, J. Kruger, S. Way, P. Finch, S. Applegate, L. Watson, E. Zahle, N. Gebben, J. Bergman, E. Dessoi, J. Alexander, C. Macdonald, M. Hedlund, P. Kaup, C. Hays, W. Evans, D. Bansal, J. Curtin, J. Sturm, RAND Corp., M. Donovan, N. Corwin, M. Mangione, K. Howard, L. Deacon, G. Metts, G. Genova, R. Provost, B. Sigurjonsson, G. Fullwood, B. Walford, J. Boyd, N. De Haan, J. Gillmer, R. Williams, E. Garland, A. Leishman, A. Phan Le, R. Lovely, M. Spoto, A. Steele, M. Varenka, K. Yarbrough, A. Cornejo, D. Compos, F. Demopoulos, G. Bylinsky, J. Werner, B. Pearson, S. Thayer, T. Edris & M. Waters.

DATA AVAILABILITY

This work did not produce or use any data.

REFERENCES

- Andrae R., Schulze-Hartung T., Melchior P., 2010, arXiv, arXiv:1012.3754. doi:10.48550/arXiv.1012.3754
- Bain, L. J. and Engelhardt, M., 1992, Introduction to Probability and Mathematical Statistics, Duxbury Press.
- Barclay T., Pepper J., Quintana E. V., 2018, ApJS, 239, 2. doi:10.3847/1538-4365/aae3e9
- Beatty T. G., Gaudi B. S., 2008, ApJ, 686, 1302. doi:10.1086/591441
- Borucki W. J., Koch D., Basri G., Brown T., Caldwell D., Devore E., Dunham E., et al., 2006, ISSIR, 6, 207
- Brout D., Hinton S. R., Scolnic D., 2021, ApJL, 912, L26. doi:10.3847/2041-8213/abf4db
- Burke C. J., Christiansen J. L., Mullally F., Seader S., Huber D., Rowe J. F., Coughlin J. L., et al., 2015, ApJ, 809, 8. doi:10.1088/0004-637X/809/1/8
- Burke C. J., Catanzarite J., 2017, ksci.rept
- Carter J. A., Yee J. C., Eastman J., Gaudi B. S., Winn J. N., 2008, ApJ, 689, 499. doi:10.1086/592321
- Carter J. A., Winn J. N., 2010, ApJ, 709, 1219. doi:10.1088/0004-637X/709/2/1219
- Christiansen J. L., Clarke B. D., Burke C. J., Jenkins J. M., Barclay T. S., Ford E. B., Haas M. R., et al., 2013, ApJS, 207, 35. doi:10.1088/0067-0049/207/2/35
- Cortés J., Kipping D., 2019, MNRAS, 488, 1695. doi:10.1093/mnras/stz1300
- Dressing C. D., Charbonneau D., 2013, ApJ, 767, 95. doi:10.1088/0004-637X/767/1/95
- Fressin F., Torres G., Charbonneau D., Bryson S. T., Christiansen J., Dressing C. D., Jenkins J. M., et al., 2013, ApJ, 766, 81. doi:10.1088/0004-637X/766/2/81
- Grimmett, G. and Stirzaker, D., 2001, Probability and Random Processes, Oxford University Press.

- Grunblatt S. K., Huber D., Gaidos E., Hon M., Zinn J. C., Stello D., 2019, *AJ*, 158, 227. doi:10.3847/1538-3881/ab4c35
- Hardegree-Ullman K. K., Cushing M. C., Muirhead P. S., Christiansen J. L., 2019, *AJ*, 158, 75. doi:10.3847/1538-3881/ab21d2
- Haykin, S., 1994, *Detection of Signals in Noise*, Wiley, ISBN: 978-0470385777
- Herman M. K., de Mooij E. J. W., Huang C. X., Jayawardhana R., 2018, *AJ*, 155, 13. doi:10.3847/1538-3881/aa991f
- Hippke M., Heller R., 2019, *A&A*, 623, A39. doi:10.1051/0004-6361/201834672
- Howard A. W., Marcy G. W., Bryson S. T., Jenkins J. M., Rowe J. F., Batalha N. M., Borucki W. J., et al., 2012, *ApJS*, 201, 15. doi:10.1088/0067-0049/201/2/15
- Hsu D. C., Ford E. B., Ragozzine D., Ashby K., 2019, *AJ*, 158, 109. doi:10.3847/1538-3881/ab31ab
- Kipping D. M., 2010, *MNRAS*, 408, 1758. doi:10.1111/j.1365-2966.2010.17242.x
- Kipping D. M., Tinetti G., 2010, *MNRAS*, 407, 2589. doi:10.1111/j.1365-2966.2010.17094.x
- Kipping D. M. & Sandford E., 2016, *MNRAS*, 463, 1323. doi:10.1093/mnras/stw1926
- Kipping D. M., Teachey A., 2016, *MNRAS*, 459, 1233. doi:10.1093/mnras/stw672
- Kovács G., Zucker S., Mazeh T., 2002, *A&A*, 391, 369. doi:10.1051/0004-6361:20020802
- Haykin, S., 1994, *Detection of Signals in Noise*, Wiley, ISBN: 978-0470385777
- Mandel K. & Agol E., 2002, *ApJL*, 580, L171. doi:10.1086/345520
- Morello G., Dyrek A., Changeat Q., 2022, *MNRAS*, 517, 2151. doi:10.1093/mnras/stac2828
- Petigura E. A., Howard A. W., Marcy G. W., 2013, *PNAS*, 110, 19273. doi:10.1073/pnas.1319909110
- Price E. M., Rogers L. A., 2014, *ApJ*, 794, 92. doi:10.1088/0004-637X/794/1/92
- Rauer H., Catala C., Aerts C., Appourchaux T., Benz W., Brandeker A., Christensen-Dalsgaard J., et al., 2014, *ExA*, 38, 249. doi:10.1007/s10686-014-9383-4
- Ricker G. R., Winn J. N., Vanderspek R., Latham D. W., Bakos G. Á., Bean J. L., Berta-Thompson Z. K., et al., 2015, *JATIS*, 1, 014003. doi:10.1117/1.JATIS.1.1.014003
- Scharf, L., 1991, *Statistical Signal Processing*, Addison-Wesley, ISBN: 978-0201190380
- Sidis O., Sari R., 2010, *ApJ*, 720, 904. doi:10.1088/0004-637X/720/1/904
- Sullivan P. W., Winn J. N., Berta-Thompson Z. K., Charbonneau D., Deming D., Dressing C. D., Latham D. W., et al., 2015, *ApJ*, 809, 77. doi:10.1088/0004-637X/809/1/77
- van Sluijs L., Van Eylen V., 2018, *MNRAS*, 474, 4603. doi:10.1093/mnras/stx3068
- Vanderburg A., Rappaport S. A., Xu S., Crossfield I. J. M., Becker J. C., Gary B., Murgas F., et al., 2020, *Natur*, 585, 363. doi:10.1038/s41586-020-2713-y
- Yao X., Pepper J., Gaudi B. S., Labadie-Bartz J., Beatty T. G., Colón K. D., James D. J., et al., 2019, *AJ*, 157, 37. doi:10.3847/1538-3881/aaf23c
- Zakamska N. L., Pan M., Ford E. B., 2011, *MNRAS*, 410, 1895. doi:10.1111/j.1365-2966.2010.17570.x

APPENDIX

This appendix provides the equations describing the light curve shape of a trapezoidal transit convolved with a top-hat i.e. a trapezoidal light curve observed with finite integration time, $g_T[t]$.

$$g_T[t] = \begin{cases} g_{T,A}[t] & \text{if } 0 < I < T_{23} < W < T_{14} \text{ and } 0 < I < (T_{14} - T_{23})/2, \\ g_{T,B}[t] & \text{if } 0 < I < T_{23} < W < T_{14} \text{ and } 0 < (T_{14} - T_{23})/2 < I, \\ g_{T,C}[t] & \text{if } 0 < T_{23} < I < W < T_{14} \text{ and } 0 < I < (T_{14} - T_{23})/2, \\ g_{T,D}[t] & \text{if } 0 < T_{23} < I < W < T_{14} \text{ and } 0 < (T_{14} - T_{23})/2 < I, \\ g_{T,E}[t] & \text{if } 0 < T_{23} < W < I < T_{14} \text{ and } 0 < (T_{14} - T_{23})/2 < I, \\ g_{T,F}[t] & \text{if } 0 < T_{23} < W < T_{14} < I \text{ and } 0 < (T_{14} - T_{23})/2 < I, \end{cases} \quad (1)$$

$$g_{T,A}[t] = \begin{cases} 1 & \text{if } t \leq (-T_{14} - I)/2, \\ 1 - \frac{\delta(2t + T_{14} + I)^2}{4I(T_{14} - T_{23})} & \text{if } (-T_{14} - I)/2 < t \leq (I - T_{14})/2, \\ 1 - \frac{\delta(2t + T_{14})}{T_{14} - T_{23}} & \text{if } (I - T_{14})/2 < t \leq (-T_{23} - I)/2, \\ \frac{\delta(4t^2 + 4t(T_{23} - I) + (T_{23} + I)^2) - 4(\delta - 1)T_{14}I - 4T_{23}I}{4I(T_{14} - T_{23})} & \text{if } (-T_{23} - I)/2 < t \leq (I - T_{23})/2, \\ 1 - \delta & \text{if } (I - T_{23})/2 < t \leq (T_{23} - I)/2, \\ \frac{\delta(4t^2 + 4t(I - T_{23}) + (T_{23} + I)^2) - 4(\delta - 1)T_{14}I - 4T_{23}I}{4I(T_{14} - T_{23})} & \text{if } (T_{23} - I)/2 < t \leq (T_{23} + I)/2, \\ \frac{\delta(2t - T_{14})}{T_{14} - T_{23}} + 1 & \text{if } (T_{23} + I)/2 < t \leq (T_{14} - I)/2, \\ 1 - \frac{\delta(-2t + T_{14} + I)^2}{4I(T_{14} - T_{23})} & \text{if } (T_{14} - I)/2 < t \leq (T_{14} + I)/2, \\ 1 & \text{if } t > \frac{T_{14} + I}{2}. \end{cases} \quad (2)$$

$$g_{T,B}[t] = \begin{cases} 1 & \text{if } t \leq (-T_{14} - I)/2, \\ 1 - \frac{\delta(2t + T_{14} + I)^2}{4I(T_{14} - T_{23})} & \text{if } (-T_{14} - I)/2 < t \leq (-T_{23} - I)/2, \\ 1 - \frac{\delta(4t + T_{14} + T_{23} + 2I)}{4I} & \text{if } (-T_{23} - I)/2 < t \leq (I - T_{14})/2, \\ \frac{\delta(4t^2 + 4t(T_{23} - I) + (T_{23} + I)^2) - 4(\delta - 1)T_{14}I - 4T_{23}I}{4I(T_{14} - T_{23})} & \text{if } (I - T_{14})/2 < t \leq (I - T_{23})/2, \\ 1 - \delta & \text{if } (I - T_{23})/2 < t \leq (T_{23} - I)/2, \\ \frac{\delta(4t^2 + 4t(I - T_{23}) + (T_{23} + I)^2) - 4(\delta - 1)T_{14}I - 4T_{23}I}{4I(T_{14} - T_{23})} & \text{if } (T_{23} - I)/2 < t \leq (T_{14} - I)/2, \\ 1 - \frac{\delta(-4t + T_{14} + T_{23} + 2I)}{4I} & \text{if } (T_{14} - I)/2 < t \leq (T_{23} + I)/2, \\ 1 - \frac{\delta(-2t + T_{14} + I)^2}{4I(T_{14} - T_{23})} & \text{if } (T_{23} + I)/2 < t \leq (T_{14} + I)/2, \\ 1 & \text{if } t > (T_{14} + I)/2. \end{cases} \quad (3)$$

$$g_{T,C}[t] = \begin{cases} 1 & \text{if } t \leq (-T_{14} - I)/2, \\ 1 - \frac{\delta(2t + T_{14} + I)^2}{4I(T_{14} - T_{23})} & \text{if } (-T_{14} - I)/2 < t < (I - T_{14})/2, \\ 1 - \frac{\delta(2t + T_{14})}{T_{14} - T_{23}} & \text{if } (I - T_{14})/2 < t \leq (-T_{23} - I)/2, \\ \frac{\delta(4t^2 + 4t(T_{23} - I) + (T_{23} + I)^2) - 4(\delta - 1)T_{14}I - 4T_{23}I}{4I(T_{14} - T_{23})} & \text{if } (-T_{23} - I)/2 < t \leq (T_{23} - I)/2, \\ \frac{\delta(4t^2 + 4t(I - 2T_{14}) + T_{23}^2)}{2I(T_{14} - T_{23})} + 1 & \text{if } (T_{23} - I)/2 < t \leq (I - T_{23})/2, \\ \frac{\delta(4t^2 + 4t(I - T_{23}) + (T_{23} + I)^2) - 4(\delta - 1)T_{14}I - 4T_{23}I}{4I(T_{14} - T_{23})} & \text{if } (I - T_{23})/2 < t \leq (T_{23} + I)/2, \\ \frac{\delta(2t - T_{14})}{T_{14} - T_{23}} + 1 & \text{if } (T_{23} + I)/2 < t \leq (T_{14} - I)/2, \\ 1 - \frac{\delta(-2t + T_{14} + I)^2}{4I(T_{14} - T_{23})} & \text{if } (T_{14} - I)/2 < t \leq (T_{14} + I)/2, \\ 1 & \text{if } t > (T_{14} + I)/2. \end{cases} \quad (4)$$

$$g_{\text{T,D}}[t] = \begin{cases} 1 & \text{if } t \leq (-T_{14} - I)/2, \\ 1 - \frac{\delta(2t+T_{14}+I)^2}{4I(T_{14}-T_{23})} & \text{if } (-T_{14} - I)/2 < t \leq (-T_{23} - I)/2, \\ 1 - \frac{\delta(4t+T_{14}+T_{23}+2I)}{4I} & \text{if } (-T_{23} - I)/2 < t \leq (I - T_{14})/2, \\ \frac{\delta(4t^2+4t(T_{23}-I)+(T_{23}+I)^2)-4(\delta-1)T_{14}I-4T_{23}I}{4I(T_{14}-T_{23})} & \text{if } (I - T_{14})/2 < t \leq (T_{23} - I)/2, \\ \frac{\delta(4t^2+I(I-2T_{14})+T_{23}^2)}{2I(T_{14}-T_{23})} + 1 & \text{if } (T_{23} - I)/2 < t \leq (I - T_{23})/2, \\ \frac{\delta(4t^2+4t(I-T_{23})+(T_{23}+I)^2)-4(\delta-1)T_{14}I-4T_{23}I}{4I(T_{14}-T_{23})} & \text{if } (I - T_{23})/2 < t \leq (T_{14} - I)/2, \\ 1 - \frac{\delta(-4t+T_{14}+T_{23}+2I)}{4I} & \text{if } (T_{14} - I)/2 < t \leq (T_{23} + I)/2, \\ 1 - \frac{\delta(-2t+T_{14}+I)^2}{4I(T_{14}-T_{23})} & \text{if } (T_{23} + I)/2 < t \leq (T_{14} + I)/2, \\ 1 & \text{if } t > (T_{14} + I)/2. \end{cases} \quad (5)$$

$$g_{\text{T,E}}[t] = \begin{cases} 1 & \text{if } t \leq (-T_{14} - I)/2, \\ 1 - \frac{\delta(2t+T_{14}+I)^2}{4I(T_{14}-T_{23})} & \text{if } (-T_{14} - I)/2 < t \leq (-T_{23} - I)/2, \\ 1 - \frac{\delta(4t+T_{14}+T_{23}+2I)}{4I} & \text{if } (-T_{23} - I)/2 < t \leq (T_{23} - I)/2, \\ 1 - \frac{\delta(2T_{14}(2t+I)-(2t+I)^2+T_{14}^2-2T_{23}^2)}{4I(T_{14}-T_{23})} & \text{if } (T_{23} - I)/2 < t \leq (I - T_{14})/2, \\ \frac{\delta(4t^2+I(I-2T_{14})+T_{23}^2)}{2I(T_{14}-T_{23})} + 1 & \text{if } (I - T_{14})/2 < t \leq (T_{14} - I)/2, \\ 1 - \frac{\delta(2T_{14}(I-2t)-(I-2t)^2+T_{14}^2-2T_{23}^2)}{4I(T_{14}-T_{23})} & \text{if } (T_{14} - I)/2 < t \leq (I - T_{23})/2, \\ 1 - \frac{\delta(-4t+T_{14}+T_{23}+2I)}{4I} & \text{if } (I - T_{23})/2 < t \leq (T_{23} + I)/2, \\ 1 - \frac{\delta(-2t+T_{14}+I)^2}{4I(T_{14}-T_{23})} & \text{if } (T_{23} + I)/2 < t \leq (T_{14} + I)/2, \\ 1 & \text{if } t > (T_{14} + I)/2. \end{cases} \quad (6)$$

$$g_{\text{T,F}}[t] = \begin{cases} 1 & \text{if } t \leq (-T_{14} - I)/2, \\ 1 - \frac{\delta(2t+T_{14}+I)^2}{4I(T_{14}-T_{23})} & \text{if } (-T_{14} - I)/2 < t \leq (-T_{23} - I)/2, \\ 1 - \frac{\delta(4t+T_{14}+T_{23}+2I)}{4I} & \text{if } (-T_{23} - I)/2 < t \leq (T_{23} - I)/2, \\ 1 - \frac{\delta(2T_{14}(2t+I)-(2t+I)^2+T_{14}^2-2T_{23}^2)}{4I(T_{14}-T_{23})} & \text{if } (T_{23} - I)/2 < t \leq (T_{14} - I)/2, \\ 1 - \frac{\delta(T_{14}+T_{23})}{2I} & \text{if } (T_{14} - I)/2 < t \leq (I - T_{14})/2, \\ 1 - \frac{\delta(2T_{14}(I-2t)-(I-2t)^2+T_{14}^2-2T_{23}^2)}{4I(T_{14}-T_{23})} & \text{if } (I - T_{14})/2 < t \leq (I - T_{23})/2, \\ 1 - \frac{\delta(-4t+T_{14}+T_{23}+2I)}{4I} & \text{if } (I - T_{23})/2 < t \leq (T_{23} + I)/2, \\ 1 - \frac{\delta(-2t+T_{14}+I)^2}{4I(T_{14}-T_{23})} & \text{if } (T_{23} + I)/2 < t \leq (T_{14} + I)/2, \\ 1 & \text{if } t > (T_{14} + I)/2. \end{cases} \quad (7)$$

This paper has been typeset from a \LaTeX file prepared by the author.